JMES The International Journal of
Mechanical Engineering and Sciences
https://iptek.its.ac.id/index.php/jmes
e-ISSN 2580-7471

Effect of Fluctuating Load on Fatigue of PPCW Flat Wagon

Teguh Suprianto[1], Achmad Syaifudin[2*], Lanang Wahyu Pamungkas[2], Julendra Bambang Ariatedja[2], Abdul Rohman Farid[3]

[1]Department of Mechanical Engineering, Politeknik Negeri Banjarmasin, Banjarmasin 70125, Indonesia

[2]Department of Mechanical Engineering, Institut Teknologi Sepuluh Nopember, Surabaya 60111, Indonesia

[3]Division of Product Supports, Indonesian Railway Company (INKA Ltd.), Madiun 63122, Indonesia

Received: 12 September 2022, Revised: 6 Desember 2022, Accepted: 10 February 2023

Abstract

Flat wagons are logistic railway vehicles that are always subjected to a heavy dynamic load. One type is the 42 ton flat wagon developed by INKA Ltd., which is well known as PPCW flat wagon. The initial design of this flat wagon was operated using a container. Nevertheless, it can operate safely without a container as well. This study was conducted to mitigate the effect of fluctuating load on fatigue of 42 ton flat wagons as cement carriers, with or without a container. The 3D flat wagon model was built and exported to ANSYS Workbench 19 to simulate the effect of the variable and mean stresses generated within the wagon. Several operational modes were applied to the model, such as an accelerated condition of 0.21 m/s^2, a constant straight track, a turn uphill track, an inclined track, a turn downward track, and a decelerated condition of 0.3 m/s^2. Transient structural, static structural, and modal analysis types are applied in the simulation consecutively to adapt the track variations. Due to the loading being dominated by compressive load, a negative stress ratio of 1.5 was utilized as the stress ratio of alternating stresses. The numerical study indicated that the straight, turn uphill, and turn downward tracks could exaggerate the stress generated due to dynamic loading. Potential fatigue failure could occur because the dynamic load produced fluctuating stresses, either alternating or mean stresses, that could damage the structural integrity of the flat wagon.

Keywords: Flat wagon, dynamic load, alternating stress, mean stress, finite element method, Soderberg

1. Introduction

Train is one of the most widely used land transportation for transporting passengers and goods. The use of trains as freight vehicles is increasing [1]. The choice of a train to transport goods is due to time and cost efficiency. The transportation of goods by railway vehicles generally used flat wagons pulled by locomotives.

A flat wagon is a railway carriage without a body and roof for transporting goods. There are four types of wagons: flat wagons, open wagons, covered wagons, and tank wagons. One of the types of flat wagons used is PPCW [2], as shown in Figure 1. The specifications of the PPCW flat wagon can be seen in Table 1. The PPCW wagon is designed for container transport. However, goods without containers are still suitable for a flat wagon. For example, in transporting cement, the container may not be used. As a replacement, the cement is placed on wooden pallets arranged along the wagon's floor, covered with tarpaulin and tied with ropes on the side frames.

The change in the use of flat wagons for transporting goods, with containers to without containers, may cause problems in the structural integrity. This problem is usually caused by changes in load distribution. In general, using a container causes concentrated loading on the structure of a flat wagon, while using pallets produces more uniform loading. It causes an abrupt change in the bending moment. The uniform load of cement in a 2 x 20-ton container provides a higher bending moment than the concentrated load type.

Many researchers in the railway vehicle field have taken the merit of numerical simulation in solving complex structural problems. Some attempted to solve the problem in the optimization of car body material or extrusion panel [3–5]. The other numerical analyses mostly discussed crash energy management, including the optimal solution for crash model shape or geometry of medium-high speed trains [6–9]. However, the mitigation study using experimental evaluation data was lacking. This investigation on PPCW flat wagon was intended to cover the research gap on that case.

*Corresponding author. Email: saifudin@me.its.ac.id

Figure 1. PPCW Flat wagon: (a) for transporting cement, (b-c) in inspection process.

Table 1. PPCW flat wagon specifications [10].

Parameter	Value
Maximum load capacity	42 ton
Maximum speed	80 kph
Shoe width	1067 mm
Axle load	15 ton
Base frame length	14600 mm
Wagon width	1438 mm
Floor height from the rail	935 mm
Coupler center height	9800 mm
Empty weight (tare)	14.5 ton

2. Method

Finite Element Method (FEM) simulation was a standard numerical procedure for solving engineering problems, such as stress analysis in structures, natural frequencies, mode shape, heat transfer, and fluid flow [11]. The analyses carried out included structural analysis, modal analysis, and transient analysis. Static structural analysis was carried out to determine the displacement, stresses, strains, and reaction forces on the structure or component of the load that did not pay attention to the effects of inertia and damping significantly. In that case, the applied load was a fixed load, and the structure's response was assumed not to change with time. Types of loading applied in the static analysis included external forces, inertial forces, non-zero displacements, and temperature for thermal strains [12]. Modal analysis was used to determine natural frequencies and mode shapes, which was the shape of the structural mode that tended to vibrate according to its frequency [13]. The modal analysis was aimed to provide design parameters to avoid resonance at a specific frequency and to determine the design in response to different dynamic loads. The transient structural analysis provided the ability to determine the system's dynamic response under each type of varying load [14].

The simulation design for this investigation was done by following three steps: i) Creating a solid model to represent the structure, ii) Running numerical simulations for the structure that was subjected to several loading conditions, and iii) Mitigating the potential problems by comparing the numerical simulation results with that of dynamic test and offering the strategic solution. The 3D solid model on a scale of 1 to 1 was built using Solidworks 2016, based on geometric information shown in Figure 2. The meshed model finally had 526,659 nodes and 142,589 elements.

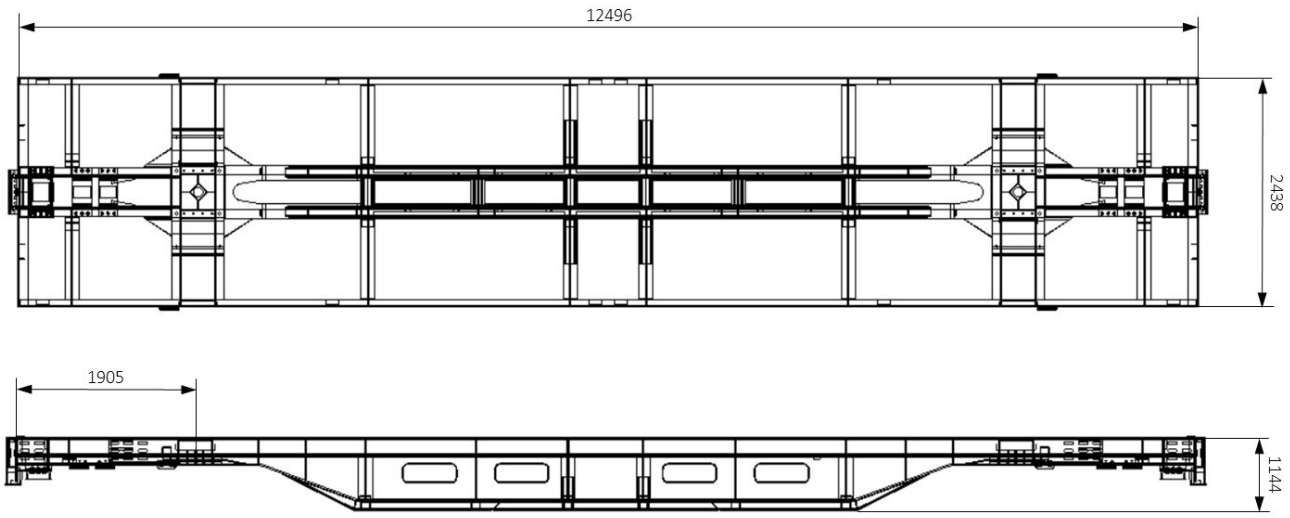

Figure 2. The main dimension of PPCW flat wagon geometry, all units in mm.

The boundary conditions used for restricting the meshed model could be seen in Figure 3. Fixed supports, indicated by the red arrow, were applied on the bolster area upon two wagon bogies. These boundary conditions were used on the lower surface of the front and rear bolsters. The main loading consisted of a vertical load acting on the upper surface of the underframe and two longitudinal loads acting on the coupler mounting area of the underframe, which were indicated by blue and green arrows, respectively.

The PPCW flat wagon underframe structure consisted of two materials, namely SS400 JIS G3101 and SS490. These technical specifications were provided by INKA Ltd. [10]. The PPCW flat wagon underframe comprised structural steel SS400 JIS G3101 for the centre sill and cross beam sections, and SS490 for the end sill and side sill sections. The properties of those materials were shown in Table 2. Connections between the components were defined as bonded contact. A bonded contact meant that the interaction between one component with another component in contact was modelled into a single rigid body. This contact treatment was done to achieve convergence in computational solid mechanics. However, it was likely unsuitable to represent the actual phenomenon of structural connections. In this numerical study, six loading variations were implemented to represent the actual loading phenomenon of a PPCW flat wagon, such as acceleration, constant straight, turn uphill, incline, turn down, and deceleration. The speeds, accelerations, turning radius, and gradient conditions for the loading variations were compiled in Table 3.

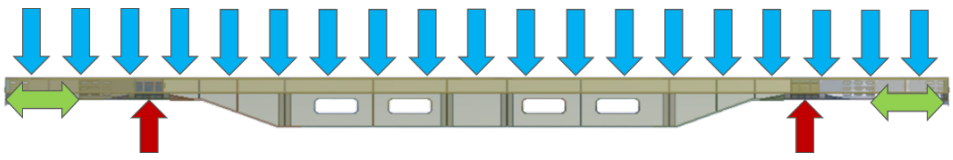

Figure 3. Boundary conditions scheme used for all loading variations.

Table 2. Material properties of SS400 JIS G 3101 and SS490 steel [15].

Property	SS400	SS490
Density (kg/m^3)	7860	7860
Tensile yield strength (MPa)	205	325
Tensile ultimate strength (MPa)	400	490
Young's modulus (GPa)	202	210
Poisson's ratio	0.3	0.3

Table 3. Conditions for loading variations.

Variation	Condition	v (km/hr)	a (m/s^2)	R (m)	Gradient
I	Acceleration	0	0.21	0	0
II	Constant straight	60	0	0	0
III	Turn uphill	60	0	800	0.0168
IV	Incline	60	0	0	0.0267
V	Turn downward	60	0	400	0.02
VI	Deceleration	60*	-0.3	0	0

*: initial velocity

Static structural analysis was used in acceleration and deceleration conditions to represent the loading variations. The longitudinal forces were obtained from the accelerated or decelerated wagon. In the meantime, transient structural analysis was applied for the wagon condition running with constant velocity, such as constant straight, turn uphill, incline and turn down. In this condition, the momentum resulting from constant velocity influenced the numerical calculation. In transient structural analysis, modal analysis was carried out to determine the mode and natural frequency of the flat wagon. The natural frequency resulting from the modal analysis was used to determine the analysis settings, such as the end time step, initial time step, minimum time step, and maximum time step used for transient structural analysis. The mode and natural frequency selected were in in 1st mode in accordance with the direction of the loads subjected to the boundary conditions. Modal analysis was carried out by considering the excitation force. Thus, the frequency resulting represented the loading.

The vertical load was derived from the maximum operational load designated for the wagon. Vertical load (P_v) is expressed by the total weight of the train (P_1) and loading weight (P_2) multiplied by the dynamic coefficient (k). Based on the technical specifications of the PPCW flat wagon, the vertical load distribution was evenly separated upon the bogie area. The equation for the vertical load was stated in Equation (1).

$$P_v = k(P_1 + P_2) \tag{1}$$

In this study, the value of k (dynamic coefficient) exceeded the standard of 1,899. This dynamic coefficient value was obtained from the research of Choi et al. [16], where the maximum load occurred when the train passed through the rail connection.

Meanwhile, the longitudinal load was derived from the total resistance. The total resistance consisted of rolling resistance (R_r), gradient resistance (R_g) and curvature resistance (R_c). The rolling resistance was the resistance that occurred between the train wheels and the rail surface. The wagon's rolling resistance formulation was shown in Equation (2), in which w was the axle weight of the bogie, A was the coefficient of 0.0085 for locomotives and 0.076 for flat wagons, and v was the speed of the train in km/hr. The curve resistance was the resistance that occurred when the train turned on the rail's curve due to friction between the wheel and the rail. The resistance on the turning rail could be formulated in Equation (3), in which G was the total weight of the locomotive and the train series, and wK was the specific bend resistance. The specific bend resistance was equal to $\frac{400}{R-20}$ [17]. The gradient resistance was the resistance that occurred when the train passed through an uphill rail line. Thus, the tractive effort or the pulling force of the wagon became heavier due to the resistance of gravity, as illustrated in Figure 4. The gradient resistance formulation could be expressed in Equation (4), in which m was the mass of the wagon, g was the gravity coefficient, and i was the track slope. The track slope or gradient was equal to $sin\,\theta$, where θ was the degree of slope.

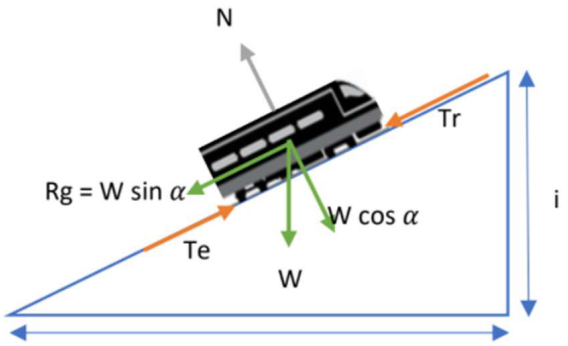

Figure 4. Gradient resistance scheme.

$$R_r = (0.6 + 13/w + Av) \times wagon\ mass \quad (2)$$

$$R_c = wK \times G \quad (3)$$

$$R_g = m\ g\ i \quad (4)$$

Thus, the total resistance for the wagon or total wagon resistance (R_t) can be expressed by Equation (5) [17]. Additional longitudinal force in acceleration and deceleration was derived from a force that acted parallel to the train, which could be obtained from Newton's third law. Equation (5) was applied to the PPCW flat wagon. The locomotive and the series of wagons behind it amounted to 20.

$$R_t = R_r + R_g + R_c \quad (5)$$

The same boundary conditions for static and transient structural analyses were applied in the numerical analysis. The difference was the initial velocity given in the transient structural analysis, which was equal to 16.6 m/s or 60 km/hour. By means of Equations (1) to (5), the resistance value for each condition was displayed in Table 4.

In this study, the carriage in the flat wagon series observed was the car behind the locomotive because it received the most significant longitudinal force among other carriages in the same series. The longitudinal forces acting on the carriage observed, either from the locomotive in the front or the car in the rear, for various loading conditions were compiled in Table 5.

In the second stage of the investigation, numerical simulations were carried out using the Fatigue Tool analysis from ANSYS Workbench 19. By utilizing the fatigue tool, fatigue analysis could be carried out simultaneously through static or transient structural analysis after adding fatigue strength data and the assumption of the stress ratio. The fatigue strength data for SS400 and SS490 were adopted from a study conducted by Morishita et al. [18] and Fumio Ogawa et al. [19]. Furthermore, the actual stress ratio should be determined through a dynamic test on the flat wagon structure. Fluctuating stress in this numerical simulation, namely the maximum and minimum stresses, was derived from the stress ratio, which was assumed to be a negative value of 1.5 due to the loading dominated by compression loads.

To assess the results of the numerical simulation, the assessment criteria used were adopted from the regulation of the Minister of Transport number KM 42 in the year 2010 concerning Standard Technical Specifications for Self-Propelling Trains [20]. The regulation required that the maximum stresses, which were maximum tensile stress or shear stress, due to the maximum load at the critical point of the train structure were 75% of the yield strength of the material. This stress value was obtained from the vertical load, which considered the tare weight and the train load. Besides, a dynamic coefficient of 1.3 should be used for loading under dynamic conditions.

The failure theories often used were Maximum Normal Stress Theory (MNST), Mohr-Colomb Theory, Maximum Shear Stress Theory (MSST), and Maximum Distortion Energy Theory (MDET) [21]. The failure theory used in this research was Maximum Distortion Energy Theory (von Mises). This failure theory predicted ductile yielding under a combination of loadings with better accuracy than other failure theories. Through the fatigue tool in ANSYS Workbench 19, stress amplitude and mean stress were obtained. The magnitude of the stress amplitude and the average working stress determined the safety of the material against fatigue failure. Fatigue failure occurred when the stress amplitude exceeded the endurance limit of the material and the maximum stress exceeded the yield strength. Several fatigue failure criteria were Soderberg, Goodman, Gerber and ASME-Elliptic. Because the material constructed PPCW flat wagon included ductile materials, the Soderberg diagram was used conservatively to determine the fatigue failure.

As the last stage of this study, the numerical analysis results were compared to dynamic test data given by the manufacturer. It was obtained from the experimental evaluation conducted by the Agency for the Assessment and Application of Technology [2]. They conducted a dynamic test using operational loading on the rail line between Arjawinangun Station – Purwokerto Station. The evaluation aimed to determine the construction behaviour of PPCW wagons under operating loads. The assessment was conducted by installing strain gauges at the points where the damage potentially occurred. The dynamic test results were evaluated using von Mises stress with a fatigue limit diagram approach based on the Soderberg criteria. By comparing point-to-point the results from the numerical simulation with that from the dynamic test, a strategic plan to mitigate the possibility of the structural failure of the flat wagon could be offered. Four points of interest in the simulation model were determined to collect the results, as the position represented the points from which the dynamic test data was collected. These points were critical stress points located around the observed maximum stress, either from numerical analysis or dynamic test.

Table 4. The total resistance for all loading conditions.

Variation	Condition	R_{loco} (kN)	R_{wagon} (kN)	R_{Tot} (kN)
I	Acceleration	7.56	69.57	77.13
II	Constant straight	10.07	277.14	287.22
III	Turn uphill	10.52	283.17	293.68
IV	Incline	10.10	277.45	287.54
V	Turn downward	10.96	289.35	300.31
VI	Deceleration	10.08	277.14	287.22

Table 5. The longitudinal force for various loading conditions.

Variation	Condition	F_{loco} (kN)	F_{car} (kN)
I	Acceleration	348.458	332.799
II	Constant straight	277.142	263.285
III	Turn uphill	283.606	269.448
IV	Incline	277.467	263.595
V	Turn downward	277.467	263.595
VI	Deceleration	-121.258	-135.115

3. Results and Discussion

The results of numerical simulations using the fatigue tool in ANSYS Workbench 19 can be shown in Figure 5 and Tables 6 to 7. The results shown are representative of all given loading variations. The results in Figure 5 and Table 6 were merely numerical simulation results, while the results in Table 7 contained a comparison between numerical simulations and dynamic tests. Comparing the simulation results with that of the dynamic test was not to validate the numerical simulation results. Conversely, this was carried out to observe the pattern or distribution tendency between them. In the case of modelling a complex structural system, numerical simulations may not be able to model it accurately. However, the numerical simulations should have an equivalent stress distribution compared to the actual phenomena.

As shown in Figure 5, the Soderberg diagram had the x-axis representing mean stresses and the y-axis representing variable stresses from dynamic loading. The Soderberg diagram was usually used to graphically represent the mean and variable stresses' influence on fatigue failure. This graphic showed that even minor mean stress could result in fatigue failure if the variable stress was too high. Conversely, combining a minor variable stress and a significant mean stress could also result in fatigue failure. The six loading conditions displayed that several points exceeded the safe area, which was found in the straight, turn uphill, and turn downward tracks. Those loading conditions needed more attention to reduce or mitigate the possibility of fatigue failure that could occur. Mitigation of potential failures that could be figured out was by strengthening the PPCW flat wagon structure or by resetting the vertical load distribution. Thus, it could be expected to reduce the amplitude and mean stress under current loading conditions. After cross-checking with the dynamic test results, it turned out that the same critical pattern also appeared. At the 1st point of interest, critical points occurred in the loading conditions under the straight, turn uphill, and turn downward tracks.

Variable stress and mean stress related to each point of interest were presented in Table 6. Through these values, corresponding life cycles could be calculated. All life cycles were obtained by using stress ratios derived from the dynamic test data. It was clear that the structure could achieve infinite life. This phenomenon may be caused by the negative stress ratio obtained from the dynamic test data, representing partially reversed variable stresses. The important thing to note from Table 6 was the magnitude of the variable stress and the corresponding mean stress. Fatigue failure was characterized by the magnitude of the two types of stress. Regarding the track, turn uphill, and turn downward tracks, the variable stress and mean stress appeared to reach values above 100 MPa and 50 MPa, respectively. The loading on these conditions also needed to be considered carefully.

Furthermore, it was necessary to compare the results of the numerical simulation with that of the dynamic test by point-to-point test results, as seen in Table 7. It was found that the highest stress value for both the dynamic test and the numerical simulation results were for loading conditions on the turn downward track. The maximum stress value from the numerical simulation was 225.34 MPa and that from the dynamic test was 257.50 MPa. The stresses in Table 7 were the equivalent stresses obtained from dynamic testing and numerical modelling, respectively. Comparing equivalent stresses was considered more appropriate for cases with complex loading conditions.

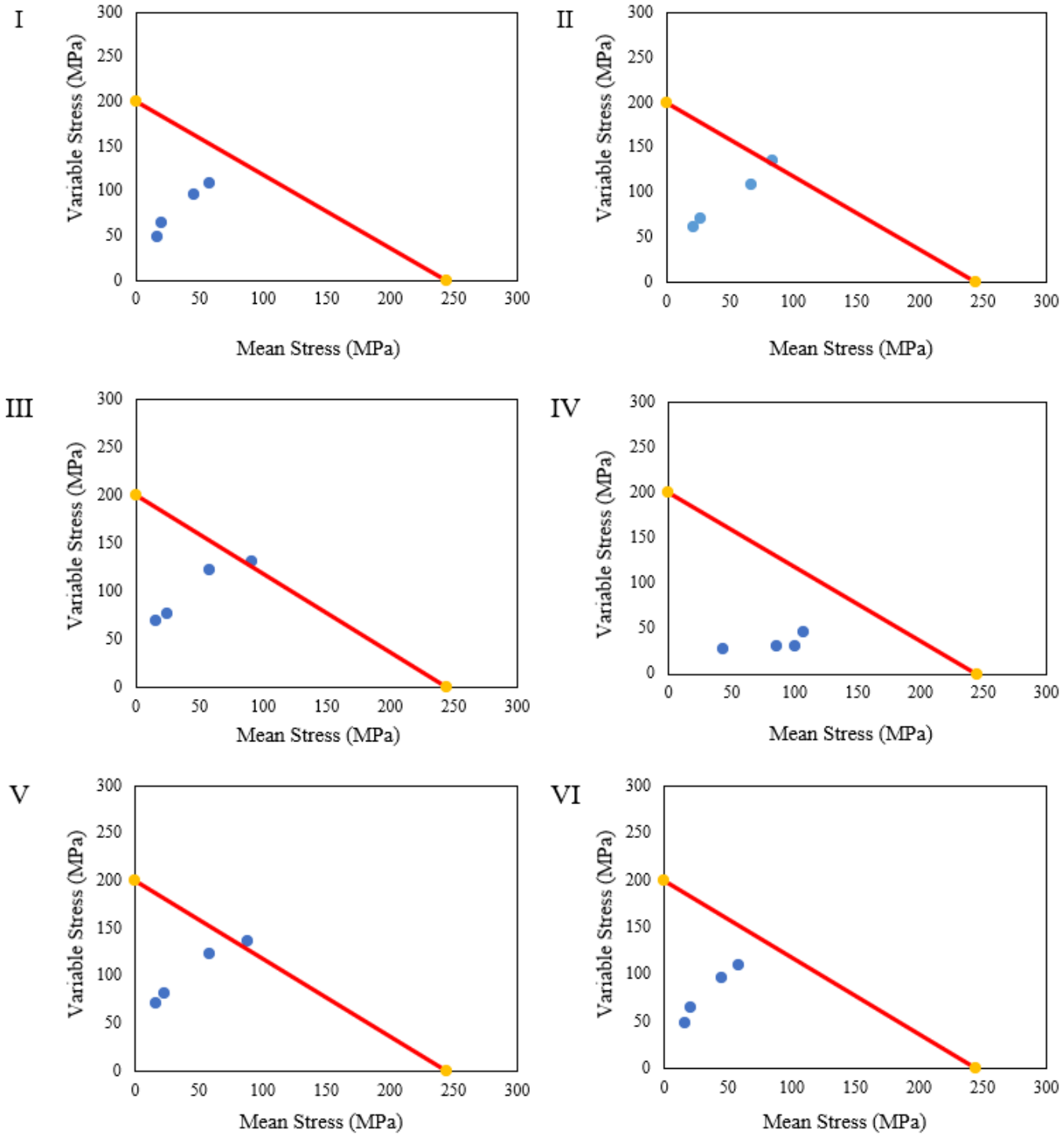

Figure 5. Soderberg diagram plotted for all loading conditions.

Table 6. Equivalent von Mises stresses.

Variation	Point of interest	Stress ratio	Variable stress (MPa)	Mean stress (MPa)	Life cycle
I	1	-0.304	109.509	58.451	10^6
	2	-0.517	64.638	20.560	10^6
	3	-0.353	96.018	45.902	10^6
	4	-0.482	48.091	16.798	10^6
II	1	-0.236	135.984	84.006	10^6
	2	-0.481	61.345	21.522	10^6
	3	-0.232	108.487	67.613	10^6
	4	-0.448	71.506	27.259	10^6
III	1	-0.181	131.236	91.037	10^6
	2	-0.632	70.027	15.799	10^6
	3	-0.356	121.658	57.792	10^6
	4	-0.505	77.212	25.408	10^6
IV	1	0.116	97.338	122.822	10^6
	2	-0.497	62.433	20.958	10^6
	3	0.003	88.062	88.668	10^6
	4	-0.246	61.821	37.441	10^6
V	1	-0.212	136.517	88.823	10^6
	2	-0.613	71.254	17.098	10^6
	3	-0.354	122.933	58.627	10^6
	4	-0.557	81.516	23.224	10^6
VI	1	0.220	65.898	103.012	10^6
	2	-0.269	46.414	26.726	10^6
	3	0.097	50.258	61.072	10^6
	4	-0.151	38.298	28.271	10^6

There are several things to note when comparing equivalent stresses from numerical simulation results with that from dynamic test results. The stress value resulting from the dynamic test was the stress obtained from measurements using a strain gauge. To obtain the equivalent stress, three strain gauges were installed in a rosette configuration to represent the strain in the three axes of the cartesian coordinates. Furthermore, Equations (6) and (7) could be used to obtain the equivalent stress.

$$\sigma_{1,2} = \frac{E}{2}\left[\left(\frac{\varepsilon_a + \varepsilon_c}{1-\nu}\right) \pm \frac{\sqrt{2}}{1+\nu}\sqrt{(\varepsilon_a+\varepsilon_b)^2 + (\varepsilon_b+\varepsilon_c)^2}\right] \tag{6}$$

$$\sigma_{eq} = \sqrt{(\sigma_1^2 + \sigma_2^2 - \sigma_1\sigma_2)} \tag{7}$$

where ε_a,ε_b, and ε_c represented strain direction a, b, and c, respectively. σ_1 and σ_2 were main stress or principal stress.

The equivalent stress from the simulation data acquired from the transient structural analysis was shown in the software in an easy-to-read manner. The difference to note between the simulation and dynamic test results were related to the variable stress. While the numerical simulation's variable stress heavily relied on the stress ratio utilized as its initial input, the dynamic test's variable stress was solely the product of measured data. A negative stress ratio was considered because compressive loads made up the majority of the load in this study.

The variable stress value difference between the simulation results and the experimental results affected the maximum stress value. This difference in value was due to conditions during train operation, which cannot be described precisely through numerical simulations. In this simulation, the dynamic coefficient obtained from the impact factor on the rail connection according to the test by Jun et al. [16], while in actual conditions, the dynamic coefficient value may exceed or less than the dynamic coefficient being used during the simulation due to differences in the type of connection or defects in the rail. However, the pattern of maximum stress distribution between the numerical simulation and the dynamic test had similarities, which occurs in loading cases on the straight, turn uphill, and turn downward tracks.

This numerical study indicated that the frame structure of the PPCW flat wagon met the static and dynamic safety criteria. Although, certain conditions needed to give more attention to avoid the potential for fatigue failure. The findings of this study were consistent with the work of Syaifudin and Ariatedja [22], who stated that there were two crucial steps to follow to lower the mean stress and variable stress values, which were strengthening the PPCW flat wagon's centre sill area, and distributing the

Table 7. Comparison between numerical and experimental results.

Variation	Point	Dynamic test			Numerical simulation		
		Equivalent stress (MPa)			Equivalent stress		
		Amp.	Mean	Max.	Amp.	Mean	Max.
I	1	126.8	67.68	194.48	109.509	58.451	167.960
	2	71.9	22.87	94.77	64.638	20.560	85.198
	3	121.2	57.94	179.14	96.018	45.902	141.920
	4	100.2	35.00	135.2	48.091	16.798	64.889
II	1	126.1	77.9	204	135.984	84.006	219.990
	2	77.4	27.14	104.5	61.345	21.522	82.867
	3	92.9	57.93	150.88	108.487	67.613	176.100
	4	114.4	43.61	158.01	71.506	27.259	98.765
III	1	144.1	99.96	244.06	131.236	91.037	222.273
	2	110.5	24.93	135.43	70.027	15.799	85.826
	3	125.4	59.57	184.97	121.658	57.792	179.450
	4	125.2	41.2	166.4	77.212	25.408	102.620
IV	1	78.9	99.67	178.66	97.338	122.822	220.160
	2	72.1	24.21	96.33	62.433	20.958	83.391
	3	58.2	58.59	116.78	88.062	88.668	176.730
	4	68.9	41.74	110.66	61.821	37.441	99.262
V	1	156	101.5	257.5	136.517	88.823	225.340
	2	111.6	26.78	138.38	71.254	17.098	88.352
	3	126.4	60.28	186.68	122.933	58.627	181.560
	4	146.4	41.71	188.11	81.516	23.224	104.740
VI	1	61.5	96.09	157.56	65.898	103.012	168.910
	2	38.9	22.44	61.41	46.414	26.726	73.140
	3	48.2	58.56	106.75	50.258	61.072	111.330
	4	57.3	42.29	99.58	38.298	28.271	66.569

load so that it was not concentrated in the space between the bogies.

The following mitigation actions, which were attainable in practice, were required to increase the acceptability of the dynamic security criteria: i) Increasing the area moment of inertia of the PPCW flat wagon's main frame. This could be done by adding a curved U-profile plate to the bottom of the main frame structure, especially in the area between the two bogies, and ii) Adjusting the load placement position to improve the load distribution subjected to PPCW flat wagon's structure. The loads should be arranged to be evenly distributed over the two bogies by reducing the load in the area between the two bogies and simultaneously maintaining the vertical distance of the load by adding a spacer. Adding a spacer between the load above the two bogies could maintain the load rigidity, thereby reducing repetitive loads or alternating stresses generated when passing through the straight, turn uphill, and turn downward tracks. From both results, the turn downward track represented the worse loading condition that generated extreme value, either alternating or mean stress.

4. Conclusion

The numerical study of the PPCW flat wagon using fatigue analysis was performed. Several loading conditions following track variation were implemented in the simulation. It can be concluded that track variation influenced the loading condition on the PPCW flat wagon. From all track variations considered, the straight, turn uphill, and turn downward tracks could generate an extreme value of alternating and mean stress. It also led to fatigue failure potential. To figure out this problem, the PPCW flat wagon manufacturer could strengthen the main frame's structure by increasing the cross-sectional area moment of inertia or resetting loading distribution between the bolster area.

References

[1] M. Minn, S. Brady, J. Cidell, K. Ratner, and A. Goetz, "Shared-use rail corridors: A comparison of institutional perspectives in the United States and The European Union," *Transport Reviews*, vol. 42, no. 3, pp. 384–407, 2022.

[2] M. Gozali *et al.*, "Failiure analysis of 'PPCW' 42 ton flat wagon under operation loads," *Jurnal Material Komponen dan Konstruksi*, vol. 15, no. 2, pp. 1–8, 2015.

[3] H.-A. Lee, S.-B. Jung, H.-H. Jang, D.-H. Shin, J. U. Lee, K. W. Kim, and G.-J. Park, "Structural-optimization-based design process for the body of a railway vehicle made from extruded aluminum panels," *Proceedings of the Institution of Mechanical Engineers, Part F: Journal of Rail and Rapid Transit*, vol. 230, no. 4, pp. 1283–1296, 2016.

[4] W. G. Lee, J.-S. Kim, S.-J. Sun, and J.-Y. Lim, "The next generation material for lightweight railway car body structures: Magnesium alloys," *Proceedings of the Institution of Mechanical Engineers, Part F: Journal of Rail and Rapid Transit*, vol. 232, no. 1, pp. 25–42, 2018.

[5] J.-S. Kim, J.-C. Jeong, and S.-J. Lee, "Numerical and experimental studies on the deformational behavior a composite train carbody of the Korean tilting train," *Composite Structures*, vol. 81, no. 2, pp. 168–175, 2007.

[6] Y. Peng, W. Ma, S. Wang, K. Wang, and G. Gao, "Investigation of the fracture behaviors of windshield laminated glass used in high-speed trains," *Composite Structures*, vol. 207, pp. 29–40, 2019.

[7] S.-W. Han and H.-S. Jung, "Weight reducing of aluminum extrusion profiles of a railway-car body based on topology and size optimization," *Transactions of the Korean Society of Mechanical Engineers A*, vol. 35, no. 2, pp. 213–221, 2011.

[8] A. Syaifudin, E. M. Nurfadillah, A. R. Farid, and A. Windharto, "Strength consideration on car body of light rail transit making from aluminum extrusion," in *IOP Conference Series: Materials Science and Engineering*, vol. 1034, p. 012025, IOP Publishing, 2021.

[9] A. Syaifudin, A. Windharto, A. Setiawan, and A. R. Farid, "Energy absorption analysis on crash-module shape and configuration of medium-speed train," in *Recent Advances in Renewable Energy Systems: Select Proceedings of ICOME 2021*, pp. 171–179, Springer, 2022.

[10] "Gerbong datar (PPCW)," *PT INKA (Persero), 2017. [Online]. Available: https://www.inka.co.id/product/view/15. [Accessed: 14-Jun-2022]*.

[11] ANSYS, "ANSYS Static Structural Theory Guide," 2012.

[12] E. P. POPOV, *Engineering mechanics of solids*, pp. 1–395. 1990.

[13] S. Deng, X. Han, and L. Yang, "Modal analysis and optimization of bus body structure," in *Journal of Physics: Conference Series*, vol. 1074, p. 012048, IOP Publishing, 2018.

[14] A. H. Kishan and P. Kondalarao, "Transient structural analysis of electric bus chassis frame," in *IOP Conference Series: Materials Science and Engineering*, vol. 1185, p. 012038, IOP Publishing, 2021.

[15] JIS, *JIS handbook: Ferrous Materials and Metallurgy*. 2012.

[16] J.-Y. Choi, S.-W. Yun, J.-S. Chung, and S.-H. Kim, "Comparative study of wheel–rail contact impact force for jointed rail and continuous welded rail on light-rail transit," *Applied Sciences*, vol. 10, no. 7, p. 2299, 2020.

[17] J. M. Valentino, "Analisa resistance, tractive effort dan gaya sentrifugal pada kereta api Taksaka di tikungan Karanggandul," *FLYWHEEL: Jurnal Teknik Mesin Untirta*, vol. 2, no. 1, 2015.

[18] T. Morishita, T. Takaoka, and T. Itoh, "Fatigue strength of SS400 steel under non-proportional loading," *Frattura ed Integrità Strutturale*, vol. 10, no. 38, pp. 289–295, 2016.

[19] F. Ogawa, Y. Shimizu, S. Bressan, T. Morishita, and T. Itoh, "Bending and torsion fatigue-testing machine developed for multiaxial non-proportional loading," *Metals*, vol. 9, no. 10, p. 1115, 2019.

[20] "Peraturan menteri perhubungan Republik Indonesia nomor KM 44 tahun 2010 tentang standar spesifikasi teknis peralatan khusus," 2010.

[21] J. L. González-Velázquez, *A Practical Approach to Fracture Mechanics*. Elsevier, 2020.

[22] A. Syaifudin and J. Ariateja, "Penanganan kasus GD 42 ton : Analisis penyebab kerusakan," Tech Report, Institut Teknologi Sepuluh Nopember, 2019.